Frequency downshifting and trapping of an electromagnetic wave by a rapidly created spatially periodic plasma

James Faith, S. P. Kuo, and Joe Huang
Department of Electrical Engineering, Polytechnic University, Farmingdale, New York 11735
(Received 17 June 1996)

Experimental and numerical results of the interaction of electromagnetic waves with rapidly time varying spatially periodic plasmas are presented. It is shown that a number of Floquet modes, each with their own oscillation frequency, are created during the interaction. Included among these modes are downshifted waves which will not exist in the single slab case, and also waves with a larger upshifted frequency than one can obtain with a single plasma layer of the same density. In addition, the periodic structure is characterized by pass and stop bands that are different from those of a single plasma layer, and the frequencies of the downshifted modes falling in the stop band of a single plasma layer. Therefore these waves are trapped within the plasma structure until the plasma decays away. To show this phenomenon a chamber experiment is conducted, with the periodic plasma being produced by a capacitive discharge. The power spectrum recorded for waves interacting with the plasma shows vastly improved efficiency in the downshift mechanism, which the numerical calculations suggest is related to the trapping of the wave within the plasma. Reproducible results are recorded which are found to agree well with the numerical simulation. [S1063-651X(97)11501-X]

PACS number(s): 52.35.−g, 52.40.Db, 52.70.Gw, 41.20.Jb

I. INTRODUCTION

When an electromagnetic wave is incident upon a spatial discontinuity that is time invariant (for instance, a dielectric half space), it is well known that its angular frequency ω will be conserved. However, since the index of refraction on either side of the boundary is different, the transmitted and reflected waves must have different wavelengths λ to maintain the same frequency [1]. Similarly, if the wave propagates through spatially homogeneous media but experiences a temporal discontinuity, it is the wavelength (or wave number $k=2\pi/\lambda$) that must be conserved. As the medium now has different indices of refraction before and after the time discontinuity, the wave frequency will now be altered [2,3]. The ability to alter the spectrum of an electromagnetic wave has many potential applications, including the extension of the range of operation of existing microwave sources and conversion of cw sources into broadband pulse sources.

If the medium the electromagnetic wave propagates through is a rapidly (on the order of a wave period) created plasma slab whose width is greater than a few free space wavelengths, the angular frequency ω_0 of the preexisting monochromatic wave will be upshifted to the new frequency [4,5] $\omega=(\omega_0^2+\omega_p^2)^{1/2}$, where $\omega_p^2=N_0e^2/m_e\varepsilon_0$ is the electron plasma frequency, N_0 is the electron density, e is the magnitude of the electron charge, m_e is the electron mass, and ε_0 is the permittivity of the free space. This upshifting to a new frequency occurs as the wavelength $\lambda_0=2\pi/k_0$ remains invariant during the temporal discontinuity, but the wave within the plasma must obey the dispersion relation for an electromagnetic wave propagating in a uniform unmagnetized plasma medium: $\omega=(\omega_p^2+k_0^2c^2)^{1/2}=(\omega_p^2+\omega_0^2)^{1/2}$.

The frequency shift phenomenon was originally observed in a laser-matter interaction experiment; however, the early work observed both upshifted and downshifted frequency components [6,7]. The experiment to demonstrate unambiguously the above-discussed frequency upshifting phenomenon was performed using two crossed microwave beams to create a rapidly growing plasma in their interaction region [8]. Other experiments also demonstrated the frequency shifting when the plasma was created using a laser [9] and a dc discharge [10].

There has also been theoretical work investigating this phenomenon. If one considers a step-ionized single (unmagnetized) plasma layer, the Laplace transform may be used to obtain an analytic solution for the transform of the fields everywhere in space [4,11]. The theoretical work was later extended to include a static magnetic field, in the cases of the wave propagating parallel to the static field [12], perpendicular to it [13], and finally at an arbitrary incident angle [14]. The effect of the magnetic field is to introduce additional plasma modes for the incident wave to be converted into upon interacting with the rapidly created plasma. Some of these waves may also have downshifted frequencies.

A common factor in all the previous work, both theoretical and experimental, is that only a single time varying plasma slab is considered. The present work builds on the previous by considering a rapidly created plasma that has a periodic spatial structure, whose geometry is shown in Fig. 1. When a plasma of this type is created suddenly about a preexisting initially monochromatic wave, this wave will decompose into an infinite number of Floquet modes [15] of the newly created dielectric medium, each with their own oscillation frequency and propagation constant. Thus one would expect that this configuration of plasma allows for the creation of not only upshifted modes which oscillate with frequencies greater than that of a wave interacting with a single plasma slab, but also of downshifted modes. It is noted that the frequency downshift mechanism of the present case is different from that of the previous case [16], which was identified to be caused by the collisional loss of the wave in the plasma. In addition, like all periodic structures the plasma is characterized by pass and stop bands. These are

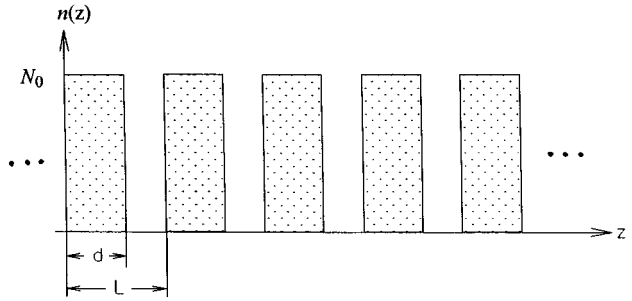

FIG. 1. Geometry of the periodic plasma structure (after plasma creation) represented by the spatial distribution of the plasma density $n(z)$.

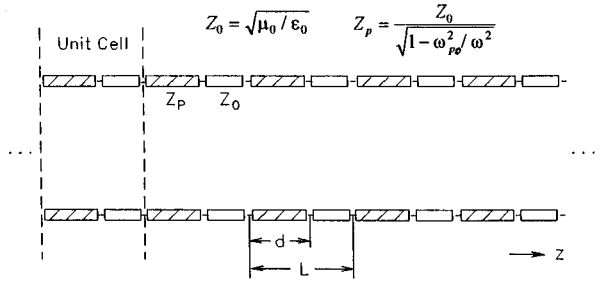

FIG. 2. Equivalent transmission line for the periodic plasma.

frequency ranges where the wave will propagate through the periodic structure (ideally) without attenuation, or the wave will be evanescent, respectively. If a wave initially exists everywhere, the cutoff modes are already inside the structure, and thus the down-shifted one, which is in the stop band of a single plasma layer has the tendency to be trapped. In the present work, we show experimentally and with numerical simulations that this trapping indeed occurs and has the effect of dramatically enhancing the efficiency of the frequency conversion process, by accumulating incident wave energy during the plasma growth period. This allows very convincing experimental results to be recorded, which are also shown to be in good agreement with numerical calculations of a wave propagating through the structure.

II. THEORY AND FORMULATION

We first calculate the dispersion relation for an electromagnetic wave propagating in an infinitely periodic dielectric medium. This results in a ''band diagram'' similar to that for electron waves in solids. It allows us to predict the frequencies of all the Floquet modes, which are expected to correspond to the peaks in the power spectrum of the resultant wave after interacting with a rapidly created periodically structured plasma. Considering the geometry of a medium like the one shown in Fig. 1, the phasor form (with $\exp[-i\omega t]$ time dependence assumed) of the wave field in the region $0 \leqslant z \leqslant L$ is written as

$$E(z) = \begin{cases} A\ \exp[ik\eta z] + B\ \exp[-ik\eta z], & 0 < z < d, \\ C\ \exp[ik(z-L)] + D\ \exp[-ik(z-L)], & d < z < L, \end{cases} \tag{1}$$

where $k=\omega/c$ and $\eta=(1-\omega_p^2/\omega^2)^{1/2}$ are the free space wave number and the index of refraction of a uniform unmagnetized plasma, respectively. By applying the boundary conditions at $z=d$ and $z=L$,

$$\begin{aligned} &E(d_-)=E(d_+), \quad \partial_z E(d_-)=\partial_z E(d_+), \\ &E(L_-)=E(L_+), \quad \partial_z E(L_-)=\partial_z E(L_+), \end{aligned} \tag{2}$$

along with the Bloch wave condition [17,18]

$$E(z)=\exp[-i\beta L]E(z+L), \tag{3}$$

where β is the propagation constant for the structure as a whole, one can derive the dispersion relation as

$$\begin{aligned} \cos(\beta L) = &\cos(k\eta d)\cos[k(L-d)] \\ &-\tfrac{1}{2}(\eta + 1/\eta)\sin(k\eta d)\sin[k(L-d)]. \end{aligned} \tag{4}$$

The frequency range covered by each branch of the dispersion curve forms a pass band, and the frequency gap between two adjacent branches of the dispersion curve forms a stop band, or band gap, which are one of the characteristic features of periodic structures. For a given βL, there exists an infinite number of Floquet modes oscillating at discrete frequencies which will be shown to correspond to the peaks in the power spectrum of the wave after interacting with a rapidly created periodically structured plasma.

The band gap feature of a periodic structure can also be revealed in terms of the equivalent impedance of the periodic structure by modeled as a transmission line, as seen in Fig. 2. If the unit cells are chosen to be symmetric, the impedance of the structure can be found by considering a bisected unit cell, shown in Fig. 3. By considering the bisection plane to be a short, we find the input impedance of the cell to be [19]

$$z_{sc} = -iZ_0 \frac{\tan[\frac{1}{2}k\eta d] + \eta\ \tan[\frac{1}{2}k(L-d)]}{\eta - \tan[\frac{1}{2}k(L-d)]\tan[\frac{1}{2}k\eta d]}, \tag{5}$$

where $Z_0=(\mu_0/\varepsilon_0)^{1/2}$ is the impedance of free space. Considering the bisection plane to be an open circuit, the input impedance is given by

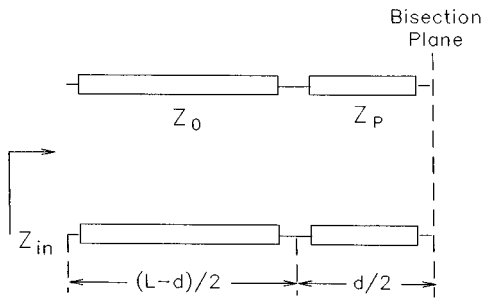

FIG. 3. Bisected unit cell of the transmission line of Fig. 2.

$$z_{oc} = -iZ_0 \frac{\eta \tan[\frac{1}{2}k(L-d)] - \cot[\frac{1}{2}k\eta d]}{\eta + \tan[\frac{1}{2}k(L-d)]\cot[\frac{1}{2}k\eta d]}. \quad (6)$$

It is noted that these two impedances are frequency dependent through both the index of refraction η and the wave number k. The total impedance of the structure normalized to Z_0 is determined from the above two quantities, and is given by

$$Z^2 = z_{oc}z_{so}/Z_0^2 = \frac{1-\eta^2 \tan^2[\frac{1}{2}k(L-d)] + \Lambda}{\eta^2 - \tan^2[\frac{1}{2}k(L-d)] + \Lambda}, \quad (7)$$

where

$$\Lambda = \eta \tan[\tfrac{1}{2}k(L-d)]\{\cot[\tfrac{1}{2}kd\eta] - \tan[\tfrac{1}{2}kd\eta]\}. \quad (8)$$

A wave of frequency ω in the plasma structure will be evanescent if the impedance is imaginary. One can show that the frequency regions with $Z^2<0$ coincide with the band with $Z^2>0$ gaps determined by the dispersion relation (4). Upon creation of the plasma, waves of many frequencies are created, and some of these waves will have very large impedances. Since the original wave initially exists in all space, so will all of the new waves. Those waves with very large impedances will be near total reflection at the structure boundaries, and are therefore *trapped* within it. This trapping phenomenon, due to the emergence of pass and stop bands (Z^2 changes sign through ∞), is new to the case of a periodic plasma, to our knowledge, although it has been investigated extensively by the laser community [20–22]. However, they have thus far been unable to demonstrate experimentally the trapping effect due to the difficulty of coupling radiation into the cutoff structure. This difficulty is not encountered in our case, and it will be shown that we create a periodic structure around the waves.

While it is intuitive to investigate an infinite periodic structure, it is more practical to investigate the case of a finite number of plasma slabs whose density varies as a function of time. Thus we need to solve the one-dimensional wave equation in an unmagnetized plasma which varies arbitrarily in both time and space,

$$\left(\frac{\partial^2}{\partial z^2} - \frac{1}{c^2}\frac{\partial^2}{\partial t^2} - \frac{\omega_p^2(z,t)}{c^2}\right)E(z,t) = 0. \quad (9)$$

The plasma density which meets the above conditions is given by

$$\omega_p^2(z,t) = \omega_{p0}^2(1-\exp[-t/\tau_r]) \times \exp[-t/\tau_f]\sum_{n=1}^{N} P_{d/2}(z-nL), \quad (10)$$

where τ_r is the plasma rise time, τ_f is the plasma decay time, $\tau_f \gg \tau_r$, $P_{d/2}(x-a)$ is a rectangular pulse of width d centered about $x=a$, L is the periodicity of the structure, $d \leqslant L$, and N is the total number of plasma slabs in the structure. To solve Eq. (9), we assume initially that a wave exists everywhere prior to the plasma creation,

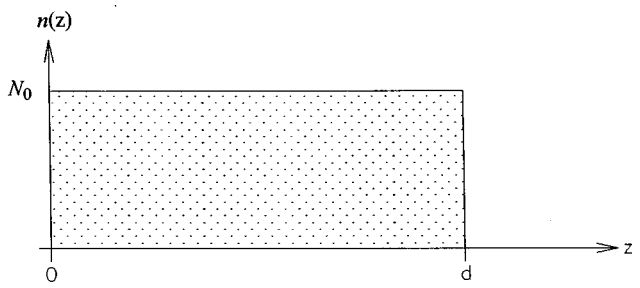

FIG. 4. Geometry of the single plasma slab.

$$E(z, t \leqslant 0) = \cos(kz - \omega_0 t). \quad (11)$$

After normalizing to dimensionless variables, we utilize a finite difference time domain method to compute the observed field (in time) at a particular spatial location. This time series is subsequently fast Fourier transformed (FFT) [23], and the power spectrum found by multiplying the time series' FFT by its complex conjugate.

III. NUMERICAL ANALYSIS

Before beginning numerical investigations into the frequency shifting of an electromagnetic wave by the periodic plasma, it is prudent to normalize all our parameters to dimensionless form. Convenient definitions of the normalized variables are

$$d/\lambda_0 \to d, \quad L/\lambda_0 \to L, \quad \omega_0 t/2\pi \to t, \quad \omega_p/\omega_0 \to \omega_p, \quad \alpha = 2\pi/\omega_0\tau_r \quad \text{and} \quad \gamma = 2\pi/\omega_0\tau_f. \quad (12)$$

For the remainder of this work we will refer to the dimensionless parameters unless units are explicitly given.

To begin our investigations, we would like to consider the case of the single plasma slab for comparison purposes, with the geometry for this case given in Fig. 4. Obviously, anything considered in Sec. II dealing with periodic media does not apply to this case. Therefore we use only the numerical solution of the wave equation (9) to analyze the single slab case. Shown in Fig. 5(a) are the power spectrum of the incident and shifted waves observed outside the plasma for the case of a slab with a width of $d=5$, an inverse rise time of $\alpha=1.0$, no decay $\gamma=0$, and a final plasma frequency of $\omega_{p0}=1.2$. Decay is not considered in this case, because we would not expect trapping of any of the time oscillating waves, as they are all upshifted to a frequency greater than the plasma frequency (the only cutoff frequency of the wave for the single slab case). The resultant spectrum shows a prominent peak centered around $\omega=1.56$, which is the value predicted by the dispersion relation $\omega=(\omega_p^2+1)^{1/2}$. Shown in Fig. 5(b) is the dependence of the field on position, taken at the instant of time four wave periods after the plasma creation. This plot, with the wave is incident from the left, shows that the shorter wavelength wave emerging from the right of the plasma slab due to frequency upshifting and the growth in field amplitude as one approaches the slab from

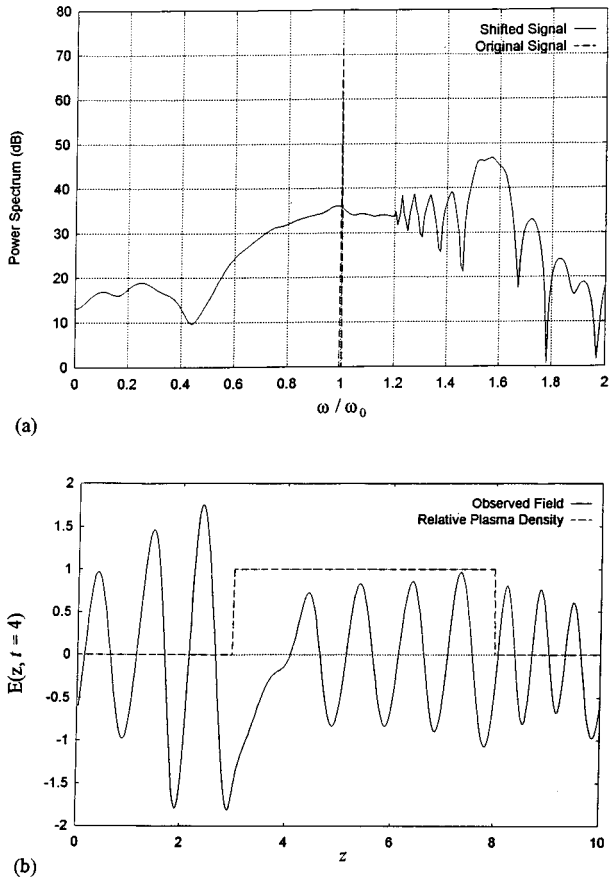

FIG. 5. Numerically computed power spectra of both the incident and shifted waves after interaction with a single plasma slab with (a) $d=5$, $\alpha=1$, $\gamma=0$, and $\omega_p=1.2$; and (b) the spatial dependence of the field at the instant of time $t=4$.

the left is due to reflection of the incident wave from the plasma. The field distribution inside the slab also shows a slight growth in wave amplitude caused by the partial reflection of the wave. Within the slab the wavelength is about the same as that of the incident wave, showing the dominance of the initial effect over that of the boundary effect for the present situation. These observations are consistent with the points discussed in Sec. I.

When considering a periodic plasma (assumed to consist of only a finite number of plasma slabs due to practical considerations) there are three broad regions of interest: the cases where L is greater than, equal to, and less than the free space wavelength of the incident wave. We shall first consider $L=1$, with the case of $L>1$ considered later in this section, and the investigation of $L<1$, deferred to Sec. IV, where this case will be covered by the simulations of our experiment.

Choosing $L=1$, $d=0.6$, and $\omega_p=1.2$, we first plot the dispersion relation (4) in Fig. 6(a), where the intersection of the curve with the $\beta L=0$ axis predicts the frequencies of the newly created modes. Shown in Fig. 6(b), the power spectrum of the wave that interacts with the plasma observed outside of a finite number ($N=10$) of plasma slabs similar to that in Fig. 1 is computed. The plasma grows rapidly with $\alpha=1$ and never decays, i.e., $\gamma=0$. Clearly apparent in the power spectrum are the upshifted peaks about $\omega=1.4$ and 2.2 as predicted by the band diagram, but one may ask what happened to the predicted downshifted mode at $\omega=0.7$. To answer this, shown in Fig. 6(c) is the power spectrum of the signal observed *inside* the plasma slabs. This plot shows upshifted modes at the same frequencies as the spectrum taken outside the structure, but it also shows the ''missing'' downshifted mode. We conclude that this downshifted mode is trapped within the periodic plasma. To explain why this occurs, shown in Fig. 6(d) is the square of the normalized impedance of the periodic structure, Eq. (7) as a function of frequency. This shows that the impedance seen by this downshifted wave is very large, meaning it cannot propagate through the boundaries of the plasma structure. Alternately, the impedance seen by the upshifted modes is relatively small, allowing the wave to propagate through the boundaries and be observed outside the plasma. The occurrence of upshifted modes that escape the plasma, and downshifted modes which are trapped, is a general feature for all our considered periodic plasmas. This trapping behavior, and how the downshifted modes escape after the plasma decays, will be discussed extensively in Sec. IV.

For the case where the plasma periodicity is greater than the free space wavelength of the incident wave, we choose $L=2.2$, $d=1$, and again $\omega_p=1.2$ with the dispersion relation of the infinitely periodic structure shown in Fig. 7(a), and the power spectrum resulting from the interaction of the wave with a finite number $N=5$ of plasma slabs observed outside the plasma structure presented in Fig. 7(b). These two plots are consistent, and show a situation qualitatively similar to that in Fig. 6(a), with the first five frequencies of the spectral peaks predicted by the dispersion relation visible in the power spectrum. It is noted that the second upshifted peak, centered about $\omega=1.7$, has a frequency greater than that of the single slab case [Fig. 5(a)]. Therefore a periodic plasma has the ability to shift the frequency of an incident microwave to greater frequencies than a single plasma slab of the same density can.

The results presented so far have shown the effect of a suddenly created spatially periodic plasma on an electromagnetic wave that propagates through it. They have shown several interesting effects when compared to the case of a single plasma slab. Among these are the possibility to shift the frequency of an electromagnetic wave to a value greater than $\omega=(\omega_p^2+1)^{1/2}$, and the creation of downshifted modes which remain trapped inside the plasma. In Sec. IV we shall show both numerically and experimentally that these trapped waves will eventually escape from the plasma as it decays.

IV. EXPERIMENTAL DEMONSTRATION OF TRAPPING AND FREQUENCY DOWNSHIFTING PHENOMENA

Shown in Fig. 8 is an overview of the experimental setup. The rapidly growing plasma is created by the discharge of a Marx bank consisting of four simultaneously fired capacitors, each rated at 1.9 μF and 60 kV. The discharge takes place between a pair of electrodes specially constructed to break down the gas in a periodic spatial pattern. Each of the electrodes consists of an aluminum sheet into which 11 2-cm-wide slots are cut, with each slot separated by 4 cm

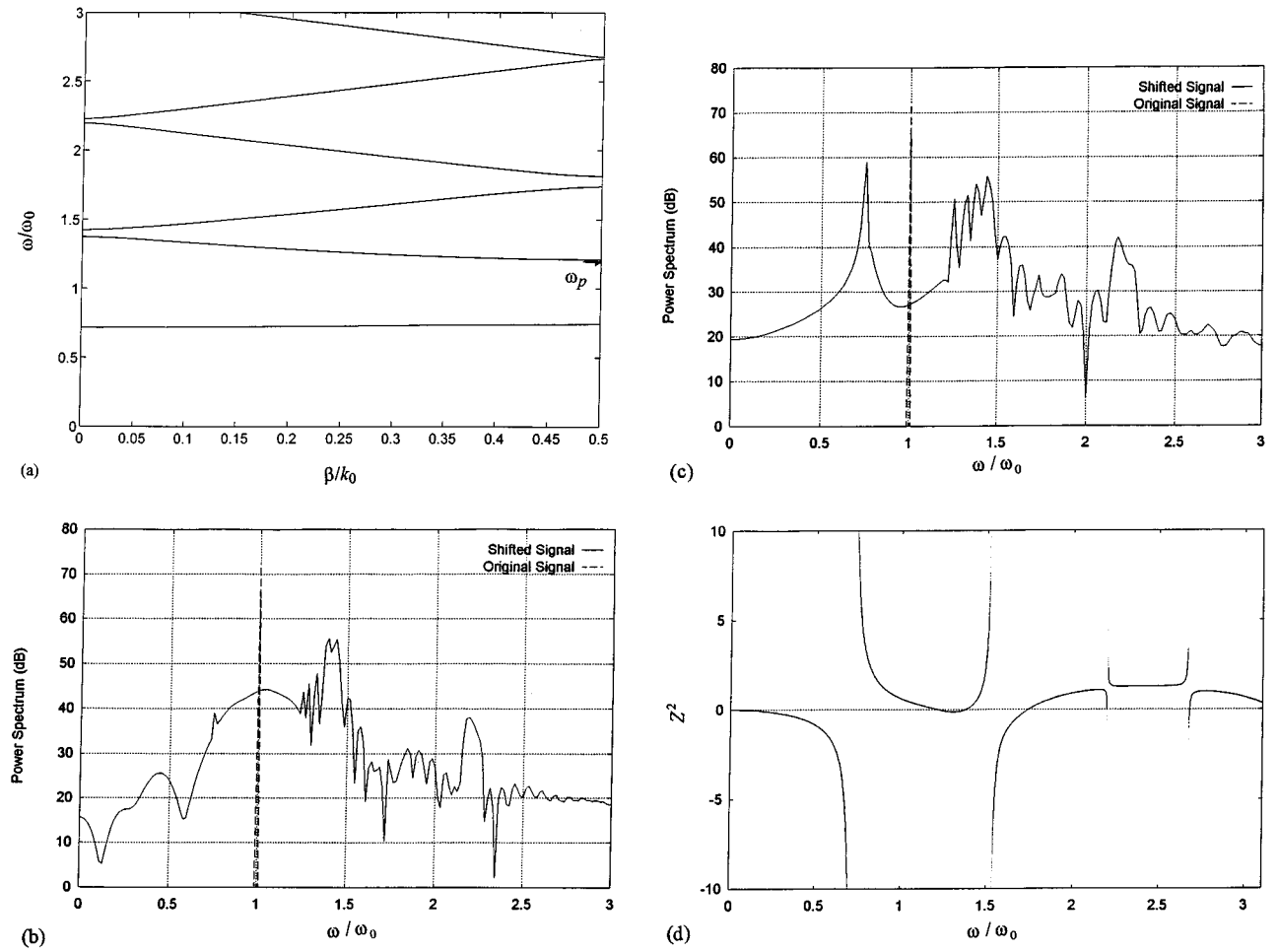

FIG. 6. Dispersion relation for a periodic plasma with (a) $L=1$, $d=0.6$, and $\omega_p=1.2$; (b) the numerically computed power spectra for the incident and shifted waves with $N=10$, $\alpha=1$, and $\gamma=0$ observed outside the plasma; (c) the power spectra observed inside the periodic structure; and (d) the functional dependence of the square of the normalized impedance on frequency.

(the total periodicity is 6 cm). These are backed by a sheet of solid copper which provides an effective guide (rather than a leaky wave antenna as the slotted sheets alone would be) for the incident cw microwave. The copper of the ground electrode also supports hundreds of small pins which facilitate the gas breakdown at their tips. The electrode structures are placed inside a vacuum chamber and suspended 16 cm apart. The chamber is a $12''\times16''\times32''$ box constructed from 1-in-thick Plexiglas, which is filled with dry air and evacuated to a pressure of about 1 torr. A photograph of the periodic plasma generated by the discharge in our vacuum chamber is shown in Fig. 9.

To perform the experiment, a cw microwave is fed into the vacuum chamber with an *S*-band horn antenna from one side. This incident signal is provided by a Hewlett Packard (HP) 692B sweep generator which provides radiation for frequencies of 2–4 GHz with mW range power. On the other side of the chamber resides another horn which collects the signal that results from the incident wave propagating through the discharge created plasma. This signal is recorded with a spectrum analyzer, HP 9105, which is later downloaded through a HP-IB port to a computer. After each of several hundred Marx bank discharges, the spectrum analyzer will sample a single point in the resultant signal's power spectrum. In addition, we would like to know the rise and fall times of the plasma density, as the trapping and downshifting phenomena depends strongly on the these times, especially that of the fall time. To record these times a Tektronix DSA 602 digital oscilloscope was used to measure the time behavior of both the current through the electrodes and the light emissions from the plasma. The scope is triggered by the discharge, and the gap current measured with a current divider which was fed through an optical isolator. The light emissions (airglow) radiated from the plasma were measured with a photomultiplier.

The typical example of the traces recorded by the spectrum analyzer which we use to estimate the plasma density rise and fall times is shown in Fig. 10. Since in order for the current to be observed there must be plasma within the electrode gap, we use the current rise time as our estimate of the plasma rise time τ_r. Once plasma is generated, the voltage across the electrodes drops considerably due to the ballasting resistor (about 40 Ω) connected in series with the plasma, for the purpose of protecting the Marx bank and also stabilizing the current flow. A quasisteady level of airglow produced by the stabilized plasma (through electron neutral collisions) is then recorded by the photomultiplier. Thus we take the fall of the airglow recorded by the photomultiplier to be the

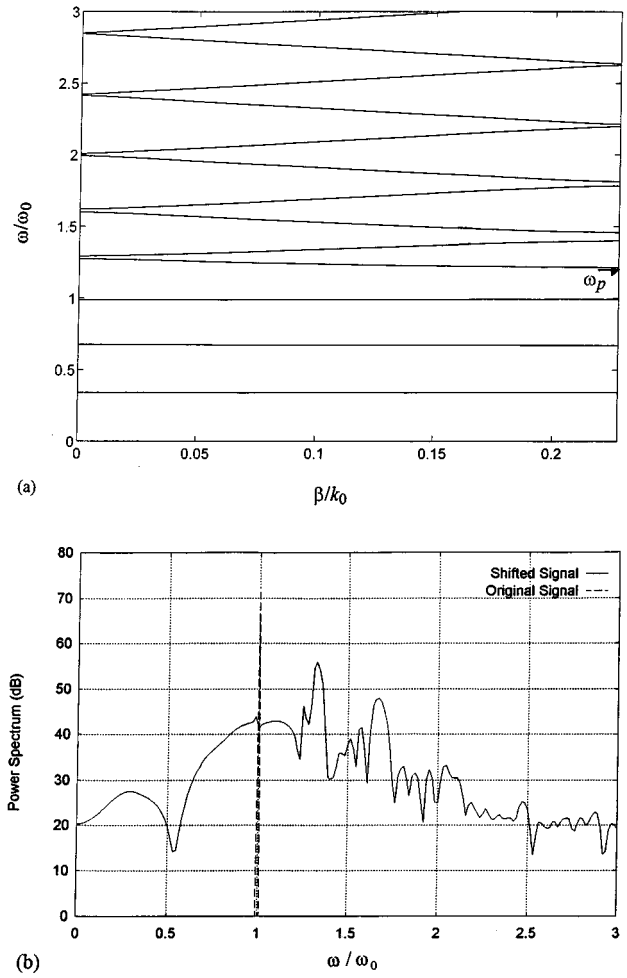

FIG. 7. Dispersion relation for a periodic plasma with (a) $L=2.2$, $d=1$, and $\omega_p=1.2$; and (b) the numerically computed power spectra for the incident and shifted waves with $N=10$, $\alpha=1$, and $\gamma=0$ observed outside the plasma.

plasma fall time τ_f, with the recurrence of airglow after the current drops to zero believed to be caused by electrons produced through detachment processes. With this in mind, we see that the figure shows ringing in the early part of the current trace. This indicates that the scope could not respond quickly enough to record the rise in the current. As this scope has a bandwidth of 1 GHz, we conclude that the current rises very quickly, on the order of nanoseconds (or less). As expected, the photomultiplier trace falls much more slowly, and can be measured directly, $\tau_f=230$ ns.

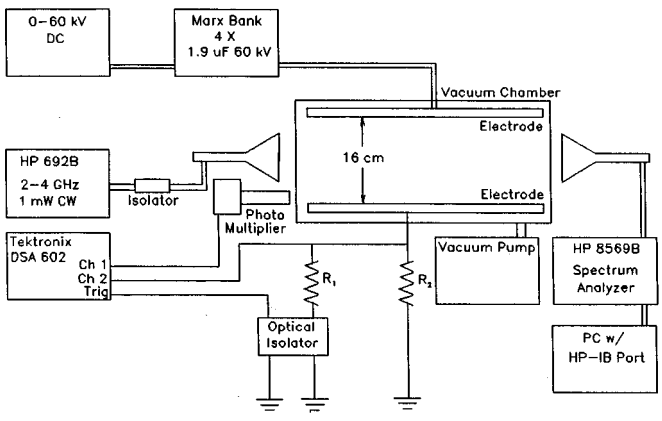

FIG. 8. A schematic of the experimental setup.

With the approximate time variation of the plasma density known, we can perform simulations which will demonstrate the trapping effect of the plasma on the downshifted modes. The simulations are performed with parameters chosen to correspond with our experimental values, with $N=11$ (and assuming a 3.1-GHz input signal), $L=0.6$, $d=0.2$, $\alpha=0.1$, and $\gamma=0.002$, with ω_{p0} estimated to be 1.2. Shown in Fig. 11(a) is the time dependence of the signal observed outside the plasma as well as the plasma frequency. In the early time portion of this plot (when the plasma frequency is large) there is a relatively large observed signal amplitude due to the upshifted waves immediately escaping from the plasma upon their creation. This is followed by a drop in the signal amplitude as all the upshifted waves propagate past the observation point, but the downshifted waves are trapped within the plasma. The small amount of signal detected is due to the tunneling of some of the wave fields through the plasma slabs. In the late time portion of the plot, when the plasma frequency has significantly decayed, the amplitude again rises, which is due to the escape of the previously trapped downshifted waves. In fact a close comparison of the observed signal with the incident signal will reveal that the early time portion does indeed contain upshifted waves, and that the late time portion contains downshifted waves. Figure 11(b) shows the power spectrum of the observed field in Fig. 11(a), as well as that of the incident signal. Finally, to explain the trapping effect, shown in Fig. 11(c) is the dependence of the square of the normalized impedance of our experimental structure on frequency for three different plasma frequencies. It is shown that as the plasma decays, the edge of the first stop band occurs at lower and lower frequencies, allowing the trapped waves to escape as the impedance seen by them becomes real.

While we have no instrument that can hope to capture the experimental time evolution of the signal after plasma creation, we can record experimental power spectra and compare them to the numerical ones. Shown in Figs. 12(a) and 12(b) are two examples of experimentally recorded power spectra with an incident frequency of 3.1 GHz and a discharge voltage of 60 kV. As this provides a dc electric field of about 3.7 kV/cm, which is well above the breakdown threshold field of 400 V/cm for 1-torr dry air [24], the maximum plasma density is not sensitive to the discharge voltage in this range. All of the recorded spectra show large downshifted components, whose envelopes show the approximately linear variation of log-scale power with frequency. Included for comparison in Fig. 12(c) are simulation results performed with the same parameters as the previous paragraph with the prominent experimental points of the two experimental traces superimposed, showing good agreement. The reproducible experimental results lead us to conclude that the periodic plasma can indeed efficiently downshift the spectral content of an electromagnetic wave, while the numerical results suggest that the trapping effect is the cause of the significant enhancement of the spectral intensity of the

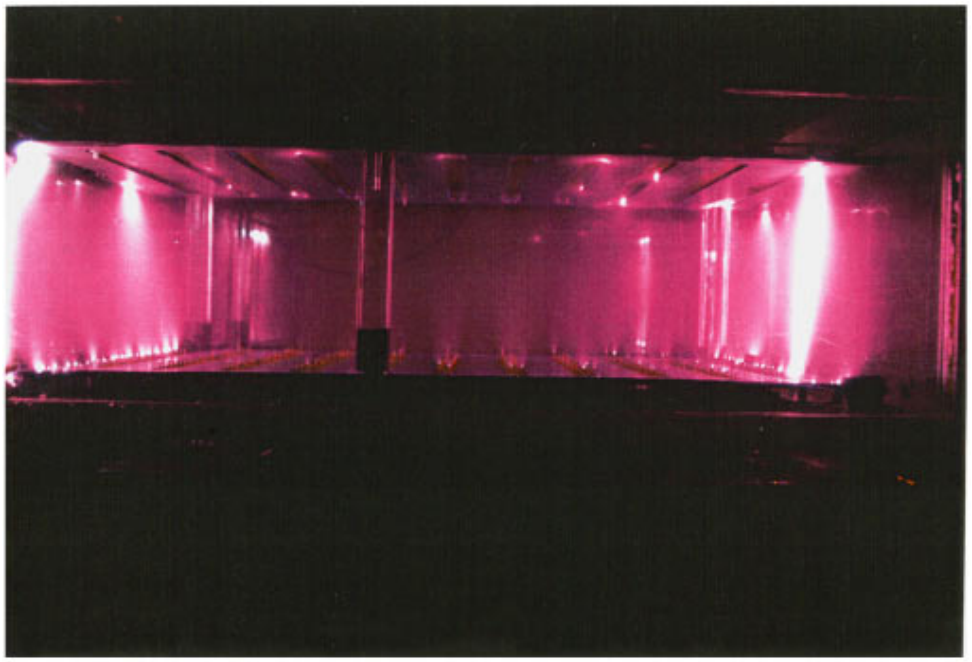

FIG. 9. A photograph of the periodic plasma layers produced by the discharge within the vacuum chamber. The chamber is a 12 in.×16 in.×32 in. Plexiglas box. The two parallel electrodes inside the chamber are suspended 16 cm apart. Each of the electrode consists of an aluminum sheet into which 11 2-cm-wide slots are cut, with each slot separated by 4 cm and backed by a copper sheet.

downshifted lines as compared to the previous experiments, with a single slab where no downshift or trapping is expected to occur [10].

V. CONCLUSIONS

We have shown that an electromagnetic wave propagating through a rapidly time varying plasma will have its spectral content altered. In addition, if the plasma also has a periodic spatial configuration, we find several interesting phenomena which happen to a wave interacting with the plasma. By proper selection of the structure periodicity and slab width, we can obtain more control over the spectrum of a wave propagating through such a plasma. Specifically, we find that the rapid creation of a periodic plasma medium provides a mechanism for the creation of downshifted waves, which relies neither on the presence of a static magnetic field nor on collisional effects, and that we can now upshift waves to frequencies greater than a single slab of the same plasma density can. Another interesting phenomenon is the ability of the plasma to trap the downshifted waves due to the impedance of the structure being large. This trapping has the practical effect of greatly enhancing the efficiency of the interaction process for the generation of frequency downshifted spectral lines.

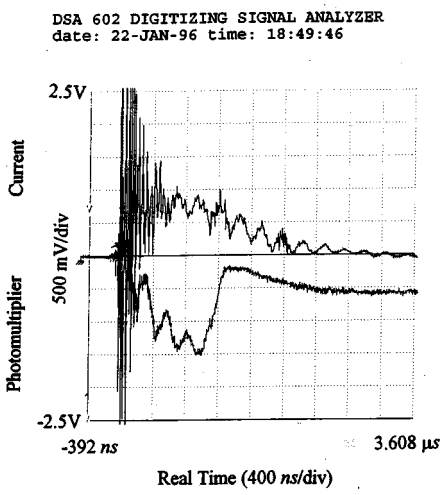

FIG. 10. Oscilloscope trace of the current across the electrodes and the air glow emissions detected by the photomultiplier for a typical discharge.

Applying Bloch's theorem, the dispersion relation for an electromagnetic wave propagating in a periodic plasma medium is derived. From this relation we can plot a band diagram showing allowed and forbidden regions for wave propagation. This allows one to predict which of the waves may propagate freely in the structure, and which will be evanescent. Since the evanescent waves are created at the same time as the plasma and exist everywhere in space, they are present inside the structure but cannot propagate. They are therefore trapped within the structure. As the plasma later decays, the initially trapped waves are able to escape the periodic structure. Numerical calculations show that the observed log-scale power of these waves as they escape from

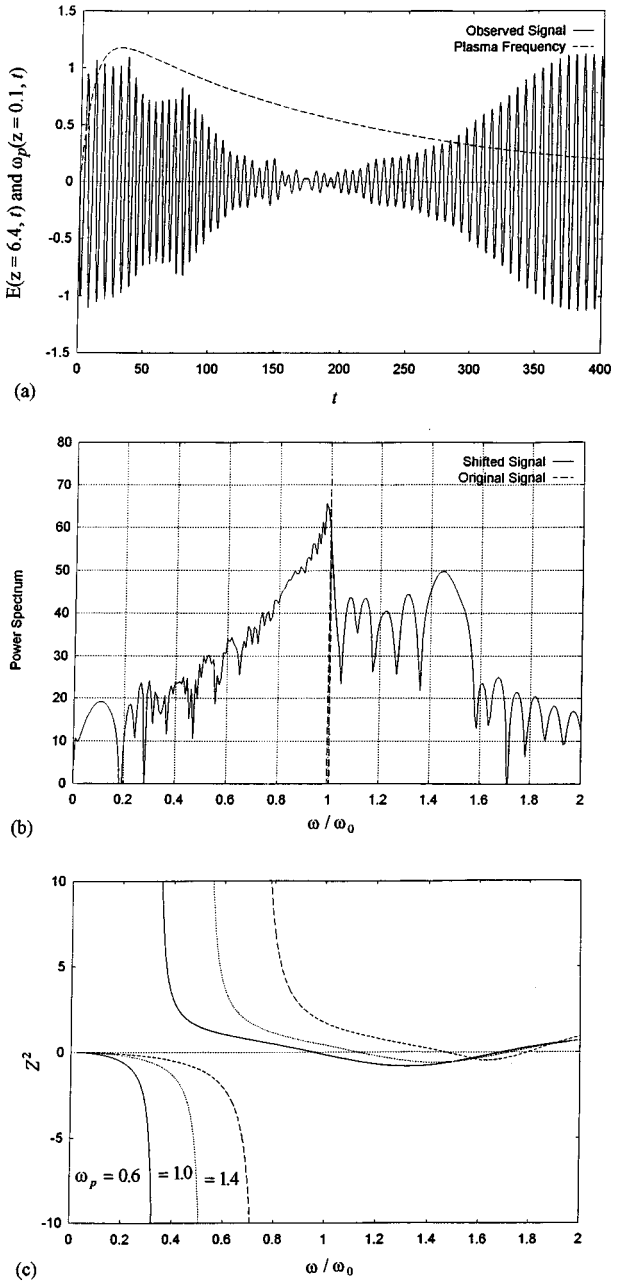

FIG. 11. Computed time evolution of the plasma frequency and the received signal observed outside the structure for (a) $N=11$, $L=0.6$, $d=0.2$, $\alpha=0.1$, $\gamma=0.002$, and $\omega_p=1.2$; (b) the power spectrum of the received signal; and (c) the square of the normalized impedance of the structure for three plasma frequencies.

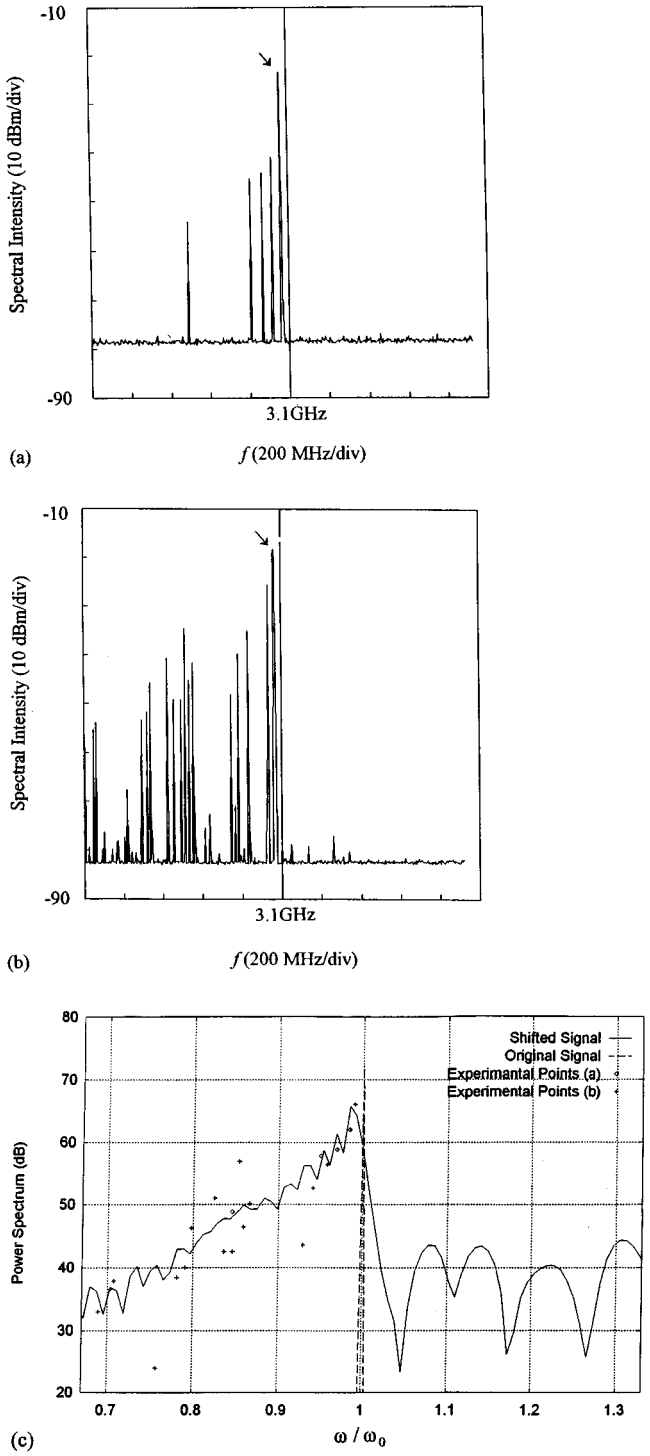

FIG. 12. Two experimentally recorded power spectra of the incident (arrowed) and downshifted signals [(a) and (b)], and (c) a simulation of the experiment with prominent experimental points superimposed. The resolution bandwidth and the sweeping speed of the spectrum analyzer are 100 kHz and 10 s/div, respectively.

the plasma structure varies almost linearly with frequency. This approximately linear dependence is also confirmed experimentally. We can therefore conclude that this trapping process is indeed the mechanism for the significant enhancement of the spectral intensity of the frequency downshifted lines.

ACKNOWLEDGMENTS

One of the authors (S.P.K.) gratefully acknowledges useful discussions with Professor G. Schmidt of Stevens Institute of Technology. This work was supported by the U.S. Air Force System Command, the Air Force Office of Scientific Research, under Grant Nos. AFOSR-F48620-92-J-0349 and -94-0076.

[1] S. Ramo, J. R. Whinnery, and T. VanDuzer, *Fields and Waves in Communication Electronics*, 2nd ed. (Wiley, New York, 1984).
[2] F. R. Morgenthaler, IRE Trans. Microwave Theory Tech. **MTT-6**, 167 (1958).
[3] L. B. Felsen and G. M. Whitman, IEEE Trans. Antennas Propagat. **AP-18**, 242 (1970).
[4] C. L. Jiang, IEEE Trans. Antennas Propagat. **AP-23**, 83 (1975).
[5] S. C. Wilks, J. M. Dawson, and W. B. Mori, Phys. Rev. Lett. **61**, 337 (1988).
[6] E. Yablonovich, Phys. Rev. Lett. **31**, 877 (1973).
[7] E. Yablonovich, Phys. Rev. Lett. **32**, 1101 (1974).
[8] S. P. Kuo, Phys. Rev. Lett. **65**, 1000 (1990).
[9] C. J. Joshi, C. E. Clayton, K. Marsh, D. B. Hopkins, A. Sessler, and D. Whittum, IEEE Trans. Plasma Sci. **PS-18**, 814 (1990).
[10] S. P. Kuo and A. Ren, IEEE Trans. Plasma Sci. **PS-21**, 53 (1993).
[11] H. L. Rappaport and C. D. Striffler, Phys. Plasmas **1**, 780 (1994).
[12] D. K. Kalluri, IEEE Trans. Antennas Propagat. **AP-37**, 1638 (1989).
[13] V. R. Goteti and D. K. Kalluri, Radio Sci. **25**, 61 (1990).
[14] M. M. Dimitrijevic and B. V. Stanic, IEEE Trans. Plasma Sci. **23**, 422 (1995).
[15] Akira Ishimaru, *Electromagnetic Wave Propagation, Radiation, and Scattering* (Prentice Hall, Englewood Cliffs, NJ, 1991).
[16] S. P. Kuo, A. Ren, and G. Schmidt, Phys. Rev. E **49**, 3310 (1994).
[17] N. W. Ashcroft and N. D. Mermin, *Solid State Physics* (Saunders College, New York, 1976).
[18] D. A. Park, *Introduction to the Quantum Theory* (McGraw-Hill, New York, 1992).
[19] R. E. Collin, *Field Theory of Guided Waves* (IEEE, Piscataway, NJ, 1991).
[20] K. M. Leung and Y. F. Liu, Phys. Rev. B **41**, 10 188 (1990).
[21] K. M. Leung and Y. F. Liu, Phys. Rev. Lett. **65**, 2646 (1990).
[22] E. Yablonovich, T. J. Gmitter, and K. M. Leung, Phys. Rev. Lett. **67**, 2295 (1991).
[23] W. H. Press, S. A. Teukolsky, W. T. Vetterling, and B. P. Flannery, *Numerical Recipes in C: The Art of Scientific Computing* (Cambridge University Press, New York, 1992).
[24] J. M. Meek and J. D. Craggs, *Electrical Breakdown of Gases* (Oxford University Press, New York, 1953), p. 84.